A new understanding of El Niño's impact over East Asia: dominance of the ENSO combination mode

Article

Published Version

It is advisable to refer to the publisher's version if you intend to cite from the work.

CentAUR

Central Archive at the University of Reading

Reading's research outputs online

A New Understanding of El Niño's Impact over East Asia: Dominance of the ENSO Combination Mode

Wenjun Zhang and Haiyan Li

Collaborative Innovation Center on Forecast and Evaluation of Meteorological Disasters,
Key Laboratory of Meteorological Disaster of Ministry of Education and ILCEC, Nanjing
University of Information Science and Technology, Nanjing, China

Malte F. Stuecker and Fei-Fei Jin

Department of Meteorology, School of Ocean and Earth Science and Technology,
University of Hawai'i at Mānoa, Honolulu, Hawaii

Andrew G. Turner

NCAS-Climate, and Department of Meteorology, University of Reading,
Reading, United Kingdom

ABSTRACT

Previous studies have shown that the Indo-Pacific atmospheric response to ENSO comprises two dominant modes of variability: a meridionally quasi-symmetric response (independent of the annual cycle) and an antisymmetric response (arising from the nonlinear atmospheric interaction between ENSO variability and the annual cycle), referred to as the combination mode (C-mode). This study demonstrates that the direct El Niño signal over the tropics is confined to the equatorial region and has no significant impact on the atmospheric response over East Asia. The El Niño–associated equatorial anomalies can be expanded toward off-equatorial regions by the C-mode through ENSO's interaction with the annual cycle. The C-mode is the prime driver for the development of an anomalous low-level anticyclone over the western North Pacific (WNP) during the El Niño decay phase, which usually transports more moisture to East Asia and thereby causes more precipitation over southern China. An atmospheric general circulation model is used that reproduces well the WNP anticyclonic anomalies when both El Niño sea surface temperature (SST) anomalies as well as the SST annual cycle are prescribed as boundary conditions. However, no significant WNP anticyclonic circulation anomaly appears during the El Niño decay phase when excluding the SST annual cycle. The analyses herein of observational data and model experiments suggest that the annual cycle plays a key role in the East Asian climate anomalies associated with El Niño through their nonlinear atmospheric interaction. Hence, a realistic simulation of the annual cycle is crucial in order to correctly capture the ENSO-associated climate anomalies over East Asia.

1. Introduction

El Niño–Southern Oscillation (ENSO) is an irregular fluctuation between warm (El Niño) and cold (La Niña) conditions in sea surface temperature (SST) over the central and eastern tropical Pacific, arising from large-scale ocean–atmosphere interactions (e.g., Bjerknes 1969; Neelin et al. 1998; Wallace et al. 1998). There is widespread public concern since ENSO gives rise to pronounced climate anomalies around the globe (e.g., van Loon and Madden 1981; Ropelewski and Halpert 1987, 1996; Trenberth and Caron 2000; Alexander et al. 2002). The significant circulation and precipitation anomalies associated with ENSO provide a potential source of predictability for forecasting regional climate anomalies on seasonal-to-interannual time scales, especially in the tropics (e.g., Charney and Shukla 1981).

Corresponding author address: Dr. Wenjun Zhang, College of Atmospheric Sciences, Nanjing University of Information, Science and Technology, Nanjing 210044, China.
E-mail: zhangwj@nuist.edu.cn

East Asia is inhabited by approximately one-third of the global population, and ENSO has been demonstrated to strongly modulate its climate (e.g., Fu and Teng 1988; Huang and Wu 1989; Zhang et al. 1996; Wang et al. 2000, 2013; Wu and Hu 2003; Lau and Nath 2006, 2009; Wu et al. 2009; Zhang et al. 2014). Positive precipitation anomalies appear commonly over the East Asian polar front extending northeastward from southern China toward southern Japan during boreal spring and early summer of the El Niño decay phase (e.g., Zhang et al. 1996; Wang et al. 2000). The low-level anticyclonic circulation anomalies over the western North Pacific (WNP) serve as a major mediator linking SST anomalies over the eastern tropical Pacific and precipitation anomalies over East Asia (e.g., Harrison and Larkin 1996; Zhang et al. 1996; Wang et al. 2000). The anomalous WNP anticyclone usually starts developing during the ENSO mature phase from boreal late autumn to winter and tends to reach its peak in the following spring season (e.g., Harrison and Larkin 1996; Wang and Zhang 2002; Wang et al. 2000, 2013). Since strong SST anomalies can be directly observed during the El Niño development, these can serve as an early indicator for subsequent precipitation and circulation anomalies to appear over East Asia.

Several dynamical mechanisms were proposed to address how ENSO affects the WNP atmospheric circulation. Diagnostic analyses by Zhang et al. (1996) suggested that the WNP atmospheric circulation anomalies are induced by suppressed convection over the western equatorial Pacific due to a weakened Walker circulation during El Niño. Wang et al. (2000) argued that cold SST anomalies over the western tropical Pacific favor the occurrence of the anomalous WNP anticyclone as a Rossby-wave response (Matsuno 1966; Gill 1980). This anomalous anticyclone can persist until early summer after the El Niño peak phase, due to a positive feedback between local surface wind and SST anomalies (wind–evaporation–SST feedback) (e.g., Wang et al. 2000). However, this mechanism was challenged by recent studies (e.g., Yang et al. 2007; Xie et al. 2009), in which the delayed Indian Ocean warming after the El Niño peak months was identified as playing an important role in the development of the anomalous anticyclone over the WNP. The delayed Indian Ocean warming can give rise to equatorial surface easterly wind anomalies and suppressed convection in the WNP region through a baroclinic atmospheric Kelvin wave response, thereby establishing the anomalous WNP anticyclone. This argument is supported by several modeling experiments (e.g., Wu and Liu 1995; Watanabe and Jin 2002, 2003; Annamalai et al. 2005; Li et al. 2005; Wu et al. 2010). A recent study

hypothesized that the delayed Indian Ocean warming is not able to fully explain the observed meridionally antisymmetric atmospheric responses over the western Pacific since the atmospheric Kelvin wave response is symmetric about the equator (Stuecker et al. 2015). So far, the fundamental dynamical mechanisms responsible for the ENSO-related climate anomalies over East Asia are still controversial and deserve further study.

As one of the latest advances in ENSO research, the so-called combination mode (C-mode) is found to occur in the Indo-Pacific region, resulting from the nonlinear atmospheric interaction between the annual cycle and ENSO variability (Stuecker et al. 2013, 2015). The C-mode encompasses both the southward shift of low-level zonal wind anomalies over the central Pacific and the development of strong low-level anticyclonic circulation anomalies over the WNP during the peak and decaying El Niño phases in boreal winter and spring. The southward shift of zonal surface wind anomalies is attributed to the meridional seasonal march of western Pacific background warm SSTs following the maximum in solar insolation (e.g., Harrison 1987; Harrison and Larkin 1998; Harrison and Vecchi 1999). The circulation anomalies associated with this are shown to accelerate El Niño event terminations by allowing the thermocline to adjust upward toward a normal state in the eastern Pacific (Harrison and Vecchi 1999; Kug et al. 2003; Vecchi and Harrison 2003, 2006; Spencer 2004; Lengaigne et al. 2006; Ohba and Ueda 2009; McGregor et al. 2012, 2013). As an important part of the C-mode, strong anticyclonic low-level circulation anomalies develop over the WNP, leading to greater fluxes of moisture toward East Asia (e.g., Stuecker et al. 2013, 2015). The annual cycle modulation is demonstrated to play a key role in the ENSO-associated atmospheric circulation and precipitation response over the WNP based on idealized model experiments and a case study for the 1997/98 El Niño episode (Stuecker et al. 2015) and hence is expected to make a dominant contribution to climate anomalies over East Asia. At present, it is unclear to what extent the annual cycle affects East Asian climate anomalies associated with ENSO in the observations, since little attention has been paid to it. This scientific issue deserves study in order to deepen our understanding of the mechanism by which ENSO affects East Asian climate.

In this study, the role of the annual cycle in ENSO-related climate impacts over East Asia will be investigated through analyses of observational data and numerical model experiments. It is our hypothesis that the annual cycle plays a predominant role in East Asian climate anomalies through its interaction with ENSO variability predominantly during the ENSO decaying

phase. In the remainder of the paper, section 2 introduces the data used, methodology, and experimental information. Section 3 illustrates the linkage of the ENSO mode and the associated C-mode to the WNP atmospheric anomalies and thus East Asian climate anomalies. In section 4, we describe the model experiments utilized to further investigate the effects of the annual cycle on the ENSO-associated climate anomalies over East Asia. The major findings and discussion are summarized in section 5.

2. Data, methodology, and experimental design

a. Data and methodology

The monthly 160-station gauge-based precipitation data (1961–2012) used here were supplied by the China Meteorological Administration. The leading wind modes associated with ENSO and the associated atmospheric circulation were investigated based on the National Centers for Environmental Prediction–National Center for Atmospheric Research (NCEP–NCAR) reanalysis (Kalnay et al. 1996). The SST data (1961–2012) were examined based on the global sea ice and sea surface temperature analyses from the Hadley Centre (HadISST1) provided by the Met Office Hadley Centre (Rayner et al. 2003). Monthly anomalies were derived relative to a 30-yr climatological mean (1971–2000), and then a 6–120-month bandpass filter was applied to each dataset since the ENSO interannual and C-mode near-annual variability are our focus. Our conclusions remain unchanged when using the unfiltered data.

Composite and linear regression analyses were employed to analyze possible impacts of ENSO and the related C-mode on the climate of East Asia. Partial correlations/regressions between atmospheric fields and the ENSO or the C-mode are used to remove the linear influence from each other by keeping the respective other index unchanged (e.g., Ashok et al. 2007). The statistical significance of our results is inferred using a two-sided Student's t test. The following eight strongest El Niño events in the available record are defined by the climate prediction center using a threshold of 0.5°C for the Niño-3.4 region (5°S–5°N, 120°–170°W) area-averaged SST anomalies: 1965/66, 1968/69, 1972/73, 1982/83, 1986/87, 1991/92, 1997/98, and 2009/10. To detect a robust signal, strong warming events only are selected given that the circulation anomalies associated with strong C-mode events usually accompany strong El Niño events (McGregor et al. 2012, 2013; Stuecker et al. 2013). Even when all El Niño events are chosen for our composite analysis, the main conclusions remain unchanged, albeit with a relatively weakened atmospheric response.

It is notable that climate anomalies over East Asia display strong seasonal differences during El Niño conditions. As an example, significant precipitation anomalies occur over southern China during El Niño decaying spring seasons (e.g., Zhang et al. 1999; Wang et al. 2000). Nevertheless, the climate signal of El Niño over eastern China is difficult to detect in summer season during its decay (e.g., Zhang et al. 1999; Wang et al. 2000), although more moisture is clearly brought to East Asia from the tropical oceans. This nonstationary behavior is possibly associated with some other modulating factors such as Tibetan Plateau snow cover and land surface conditions over Eurasia, strongly influencing the East Asian summer monsoon (e.g., Ye 1981; Tao and Ding 1981; Zhang et al. 2004; Wu and Kirtman 2007; Wang et al. 2008; Wu and Qian 2003; Wu et al. 2012). In this study, the El Niño decaying months from February to May (FMAM) are our focus since the land precipitation anomalies are most evident during this season in China. The "decaying months" can also be defined by March–May (MAM), and even March–June (MAMJ) or February–June (FMAMJ), and the qualitative conclusions remain the same.

b. Experimental information

To examine the role of the annual cycle in modulating ENSO impacts over East Asia, two sets of experiments are conducted based on the atmospheric general circulation model (AGCM) GFDL Atmospheric Model, version 2.1 (AM2.1), with a horizontal resolution of 2.5° longitude × 2° latitude with specified SST boundary conditions (Anderson et al. 2004). The specific experimental designs will be shown in section 4, which has also been described in the supplementary materials of Stuecker et al. (2013).

3. Observed analyses for linkage of ENSO and C-mode to the East Asian climate

We perform an empirical orthogonal function (EOF) analysis, as in previous studies (McGregor et al. 2012, 2013; Stuecker et al. 2013), on the surface wind anomalies over the equatorial Pacific (10°S–10°N, 100°E–80°W) to detect the spatial and temporal wind structures associated with ENSO and the C-mode. Figure 1 shows the leading two EOF modes and their associated principal components (PCs). The leading two modes, respectively, account for 23.1% and 18.0% of the total variance, and are well separated from each other based on the rule of North et al. (1982). The typical ENSO mode wind anomaly pattern is captured by the leading EOF mode (EOF1), which exhibits equatorially quasi-symmetric westerly wind anomalies occurring over the
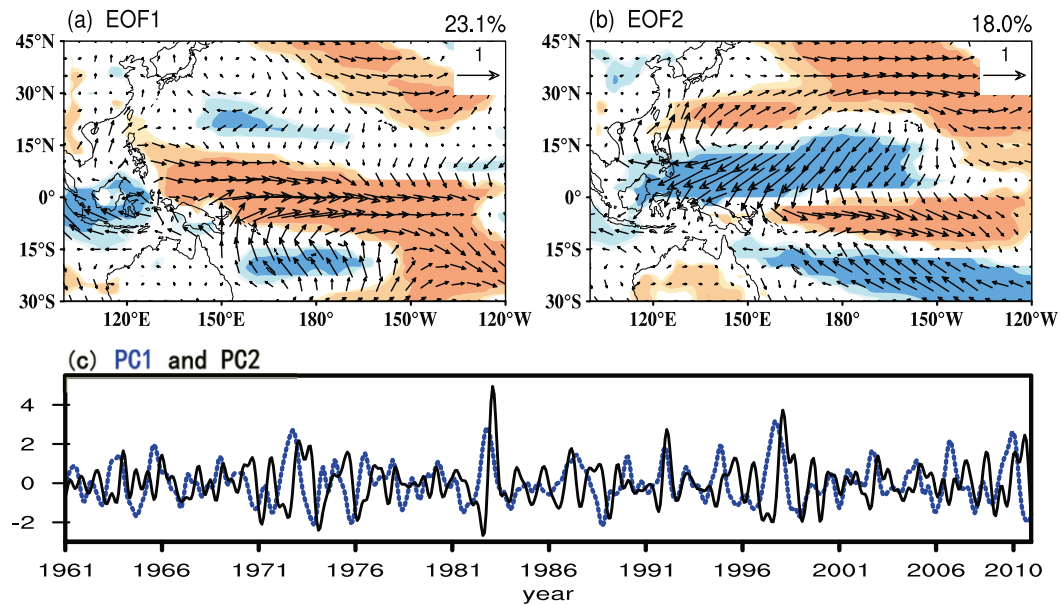
FIG. 1. (a),(b) The leading two EOF spatial patterns and (c) their corresponding normalized PC time series of surface wind anomalies (m s^{-1}) over the tropical Pacific. The EOF spatial patterns are obtained by the regression of normalized PCs on the surface wind anomalies. Light (dark) yellow and blue shadings in (a) and (b) present westerly and easterly anomalies exceeding the 90% (95%) confidence level, respectively.

central Pacific (Fig. 1a). A high correlation ($r = 0.87$) between the Niño-3.4 index and PC1 further confirms that the first EOF mode represents the direct atmospheric response associated with ENSO. Compared to EOF1, the EOF2 wind anomaly pattern displays meridionally antisymmetric wind anomalies (Fig. 1b). An anomalous anticyclone is located over the WNP and a cyclonic meridional shear of wind anomalies occurs over the central South Pacific. This wind anomaly pattern is referred to as the C-mode and arises from the interaction between the annual cycle and interannual ENSO variability (Stuecker et al. 2013, 2015). The PC2 time series can be well reconstructed by using a product of PC1 and the annual cycle of the western Pacific SSTs, as documented by Stuecker et al. (2013). The direct ENSO circulation response therefore does not include the characteristic pattern of the anomalous WNP anticyclone (Fig. 1a), the key mediator linking the tropical eastern Pacific warming and the climate anomalies over East Asia. The WNP anticyclonic circulation anomalies depicted by EOF2 suggest that the annual cycle plays a key role modulating ENSO climate impacts over East Asia. We will demonstrate this hypothesis in the remainder of the paper.

Figure 2 shows the seasonal evolution of surface wind PC1 and PC2 during the El Niño events. The composite PC1 describes a canonical El Niño evolution, with anomalies developing in summer, peaking during late autumn or winter, and decaying in the following spring.

Following the traditional definition, we choose the winter [December–February (DJF)] mean PC1 values to investigate the impacts of PC1 on the following seasonal climate anomalies over East Asia. In contrast to PC1, PC2 remains negative until September of the El Niño developing year and then reverses its sign abruptly (Fig. 2). It reaches its peak during late winter and early
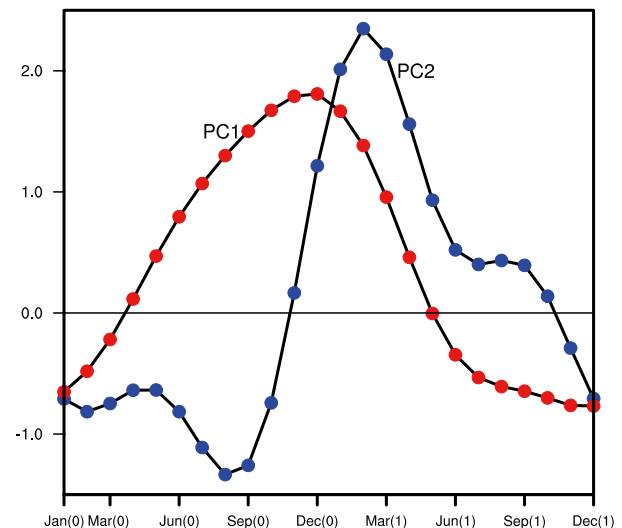

FIG. 2. Composite monthly evolution of normalized PC1 (red dotted line) and normalized PC2 (blue dotted line) for all El Niño events during the 1961–2012 period. The abscissa indicates a 24-month period from January of year 0 to December of year 1.
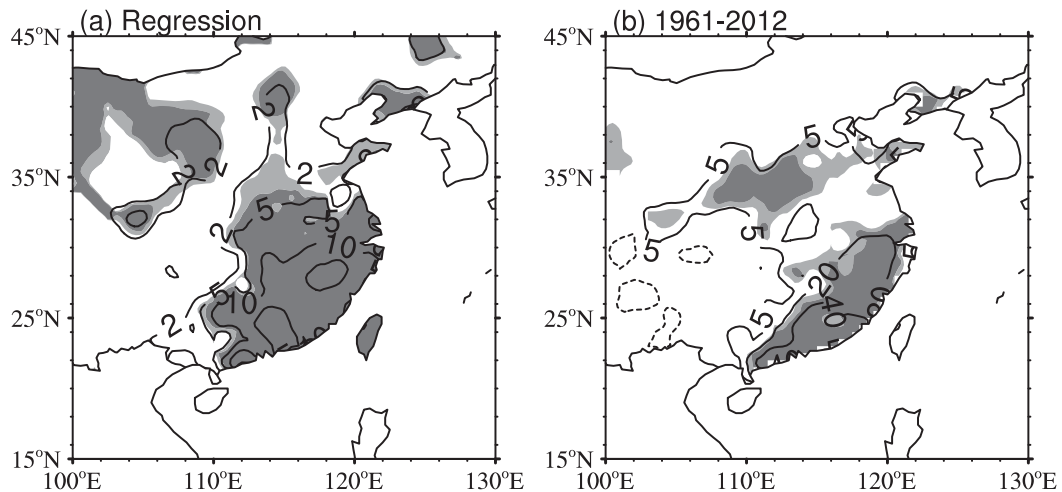
FIG. 3. (a) FMAM precipitation anomalies (contours; mm month^{-1}) regressed upon the preceding normalized DJF PC1. (b) Composite FMAM precipitation anomalies during the El Niño decaying phase for the period 1961–2012. Light (dark) shading indicates where the regression coefficient and composite values exceed the 90% (95%) confidence level.

spring, capturing a strong southward shift of the central Pacific westerly anomalies and the development of the WNP circulation anomalies (McGregor et al. 2012). PC2 enters its decaying phase during summer and early autumn following the El Niño mature phase. Compared to PC1, the peak phase of PC2 is delayed by approximately two to three months and it exhibits much faster time scales [for a discussion of the near-annual time scale, see Stuecker et al. (2013, 2015)]. Here, the season January–March (JFM) is defined as the PC2 mature phase and the JFM mean is used as a measure of the C-mode to detect its linkage to East Asian climate during the El Niño decaying phase. It is noted here that other possible definitions for the mature phases of PC1 and PC2 (e.g., by including the adjacent months) do not alter our conclusions.

To detect possible ENSO impacts on precipitation changes, Fig. 3a shows the FMAM precipitation anomalies regressed on the preceding DJF average PC1. In this study, the region of eastern China is shown as an example to illustrate the ENSO impacts on the East Asian precipitation. Following El Niño events, eastern China usually receives enhanced precipitation during its decaying phase, especially for the southern part approximately south of 35°N and east of 110°E. Furthermore, the composite precipitation anomalies over the period 1961–2012 are computed during eight strong El Niño events to confirm robustness of the precipitation response. As shown in Fig. 3b, similar precipitation anomalies are evident over eastern China (east of 105°E) despite the statistically significant anomalies being confined to southeastern China. Recently, another type of El Niño, the so-called central Pacific (CP) El

Niño, is argued to occur more frequently over the central tropical Pacific in the post-2000 period, which exhibits very different climate impacts over East Asia (Larkin and Harrison 2005; Ashok et al. 2007; Weng et al. 2007; Kao and Yu 2009; Kug et al. 2009; Yeh et al. 2009; Feng et al. 2010; Ren and Jin 2011; Zhang et al. 2011, 2013; Feng and Li 2011; Xie et al. 2012, 2014a,b; Karori et al. 2013; Xiang et al. 2013; Yuan et al. 2012; Wang and Wang 2013). We further inspect the precipitation composite for the canonical El Niño events (i.e., eastern Pacific El Niño) to test if this El Niño diversity might bias our analysis. Almost the same El Niño signal occurs in the precipitation over southeastern China when we remove the CP events (not shown). Even for CP El Niño events, such as the 1991/92 and 2009/10 events, similar positive precipitation anomalies are also evident in this region (not shown). These results suggest that El Niño events are usually accompanied by increased precipitation over eastern China, which has been mentioned by many earlier studies (e.g., Zhang et al. 1999; Wang et al. 2000).

Figure 4 shows the correlation and partial correlation between the JFM PC1 and the FMAM precipitation anomalies to detect the pure impacts of PC1. As in Fig. 4a, a statistically significant positive correlation is observed over southeastern China between the FMAM precipitation anomalies and the JFM PC1. The correlation coefficients obtain values as high as 0.5. However, almost no significant correlation is detected in this region after removal of the effects of PC2 for a partial correlation (Fig. 4b). The correlation and partial correlation techniques are also utilized to distinguish the impact of the C-mode (PC2) from the ENSO mode
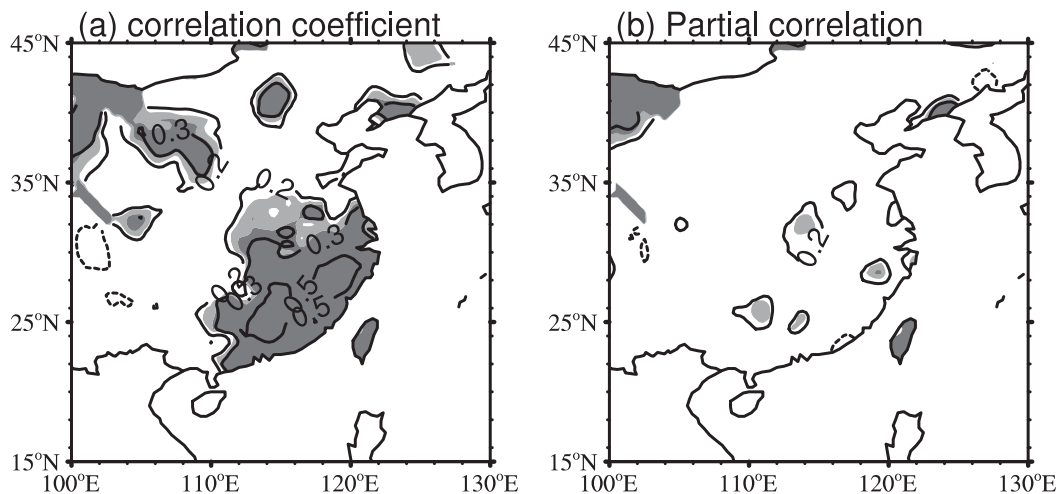
FIG. 4. (a) Correlation between the FMAM precipitation anomalies and the preceding DJF PC1 time series. (b) As in (a), but for partial correlation removing linearly the impact of the preceding JFM PC2. Light (dark) shading indicates a correlation coefficient exceeding the 90% (95%) confidence level.

(PC1). A statistically significant positive correlation between the C-mode and the precipitation anomalies is detected over southeastern China (Fig. 5a), which is not contaminated by the ENSO mode signal (Fig. 5b). These statistical relations suggest that the ENSO SST forcing itself is not able to produce more precipitation over southeastern China and its impacts on precipitation over southeastern China are only conveyed via the C-mode through the interaction of ENSO with the annual cycle. To further confirm those results, the FMAM rainfall variability is reconstructed using the simultaneous PC1 and PC2 information (Fig. 6). Almost no obvious precipitation variability is explained by the PC1 time series

alone. However, in excess of 30% of variance can be explained when further considering the PC2 time series. This highlights the importance of the C-mode.

The atmospheric teleconnection is also examined here to understand possible links between precipitation anomalies over eastern China and the two leading modes (i.e., ENSO mode and the C-mode). For the ENSO mode, there is an anomalous eastward moisture transport located on the equator, causing more precipitation over the central–eastern equatorial Pacific (Fig. 7a). The moisture transport anomalies are mainly induced by the meridionally quasi-symmetric CP westerly wind anomalies during El Niño events (Fig. 1a). No
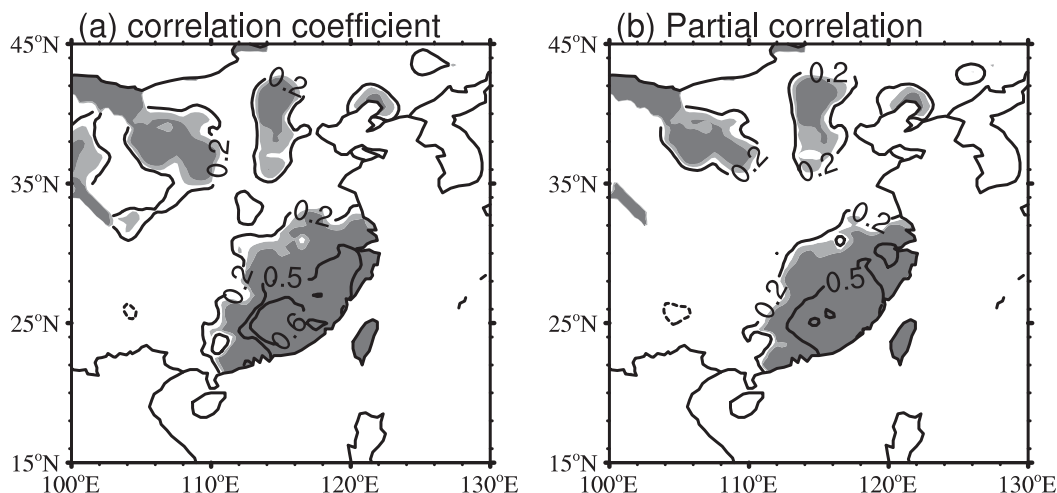

FIG. 5. (a) Correlation between the FMAM precipitation anomalies and the preceding JFM PC2 time series. (b) As in (a), but for partial correlation removing linearly the impact of preceding DJF PC1. Light (dark) shading indicates a correlation coefficient exceeding the 90% (95%) confidence level.
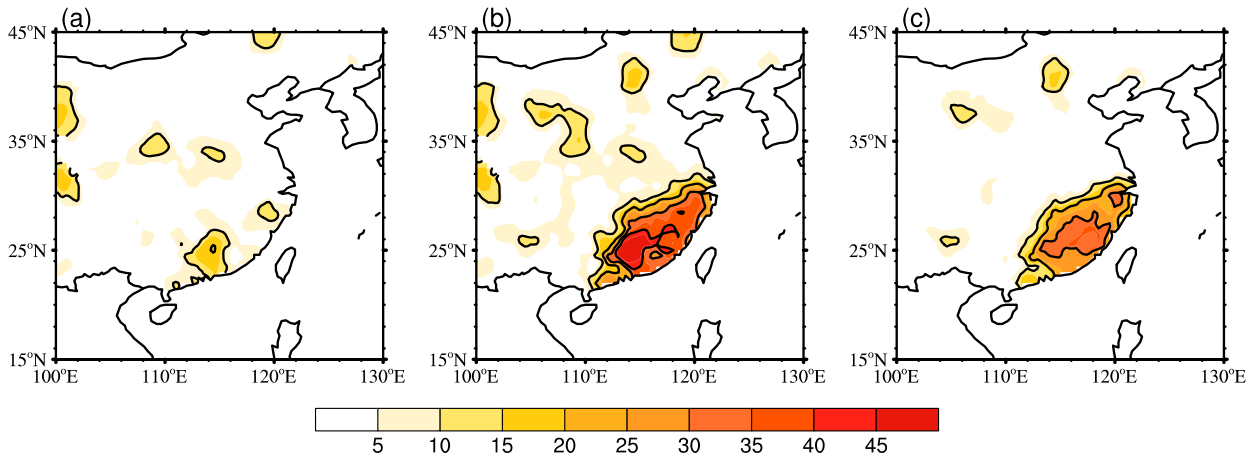
FIG. 6. Explained variance of FMAM precipitation (%) over east China by (a) the simultaneous PC1, (b) both simultaneous PC1 and PC2, and (c) their difference. The contours indicate values of 10%, 20%, 30%, and 40%.

statistically significant atmospheric anomaly occurs over the WNP (Fig. 7a). When zonally averaging the meridional circulation over 110°–120°E, one finds strong sinking motion over the equatorial western Pacific due to a weakened Walker circulation for the ENSO mode (Fig. 8a). In contrast to the ENSO mode, significant moisture transport anomalies associated with the C-mode appear over the WNP region and the central South Pacific (Fig. 7b), consistent with the surface wind EOF2 pattern (Fig. 1b). In the northwest section of the anomalous WNP anticyclone, an anomalously northeastward moisture transport prevails over southern East Asia, thereby bringing more moisture to East Asia from the deep tropics. For the meridional overturning circulation, the center of the anomalous sinking motion is shifted northward by approximately 10°N for the C-mode compared to the ENSO mode (Fig. 8b). Simultaneously for the C-mode only, statistically significant rising air anomalies appear on both sides of the equator at approximately 10°–15°S and 20°–30°N (Fig. 8b). The anomalous rising motion is much stronger north of the equator, corresponding to large precipitation anomalies

over southern China. Our statistical analyses from Figs. 4–8 suggest that the direct atmospheric response to the ENSO mode is confined to the equatorial region, modifying the zonal atmospheric circulation rather than the meridional circulation. The C-mode acts to expand the equatorial atmospheric anomalies toward off-equatorial regions. Therefore, ENSO variability itself seems to have no significant impact on the East Asian climate; rather, it may affect the East Asian climate variability through its interaction with the annual cycle of SST and lower tropospheric winds.

4. Model experiments

According to our analysis of the observational data, we summarize that ENSO without the presence of the C-mode would give rise to very different atmospheric circulation anomalies, especially over the WNP region. To verify this, two experiments were designed. In the first experiment (EX_AC), the ENSO-associated SST anomalies, obtained by the regression of monthly SST anomalies upon the normalized PC1 (Fig. 1), are
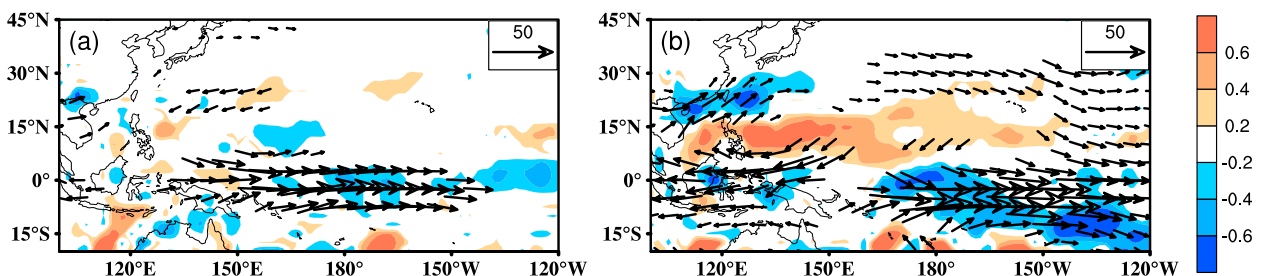

FIG. 7. Vertically integrated moisture transport anomalies (vectors; $kg\,m^{-1}\,s^{-1}$) and anomalies of its divergence (shading; $10^{-5}\,kg\,m^{-2}\,s^{-1}$) during FMAM partially regressed upon the preceding normalized (a) DJF PC1 and (b) JFM PC2. Vertical integration is performed from the surface to 300 hPa. Only values with a partial correlation coefficient exceeding the 95% confidence level are shown.
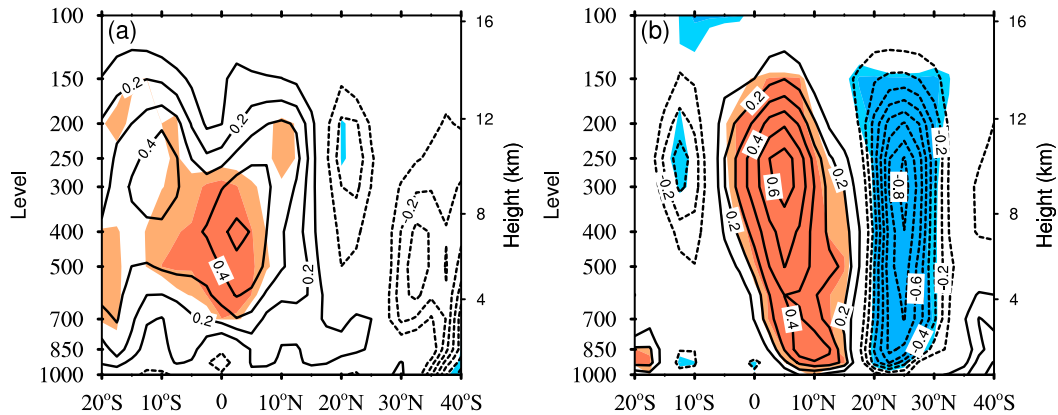
FIG. 8. Zonal mean (110°–120°E) FMAM vertical pressure velocity (contours; 10^{-2} Pa s^{-1}) partially regressed upon the preceding normalized (a) DJF PC1 and (b) JFM PC2. Light (dark) yellow and blue shadings indicate positive and negative partial correlation coefficients exceeding the 90% (95%) confidence level, respectively.

imposed on the climatological annual cycle of SST in the entire tropics (20°S–20°N). Multiplying the SST anomaly pattern by the normalized PC1 gives the spatiotemporal evolution of the SST anomaly field. SST anomalies outside of the tropical bands are set to zero. The second experiment (EX_NO_AC) has the same ENSO SST anomaly forcing but not the annual-cycle-associated meridional movements of climatological SSTs as boundary forcing. The climatological SSTs are specified as the September equinox conditions when the sun is located directly over the equator. The EX_NO_AC experiment is designed to investigate the importance of the SST annual cycle to ENSO-associated atmospheric circulation anomalies over the WNP through intercomparison with the EX_AC experiment. All simulations are integrated from 1958 to 2001, a period that covers all the observed strong El Niño events except for the 2009/10 event. We conduct a 10-member ensemble of the experiments.

Figure 9 shows the evolution of the total SST fields, with and without inclusion of the annual cycle, which are used to force the atmospheric model. The meridional movement of the central Pacific SSTs during the 1997/98 El Niño event is taken as an example to display the crucial difference arising from the two experiment designs. We choose a zonal mean region near the date line (160°W–180°) to display the SST evolution, since the ENSO SST anomalies and the background SSTs are both relatively strong here and hence can easily excite an atmospheric convection response. For the experiment including the seasonal cycle (EX_AC), the maximum SSTs are first found centered on the equator from June to October of 1997. Afterward, the maximum SSTs move abruptly into the Southern Hemisphere and become centered at about 5°S (Fig. 9a). In contrast, in the experiment excluding the SST annual cycle (EX_NO_AC), the maximum SSTs stay centered on the equator and display no meridional movement for the entire
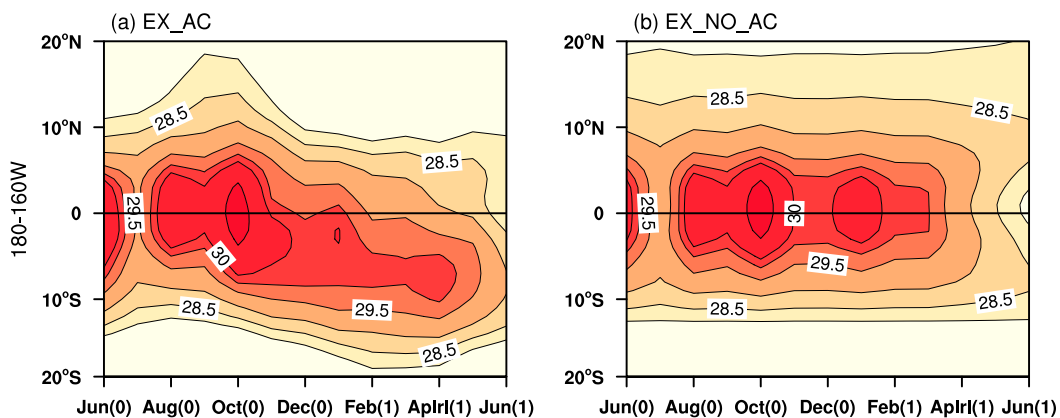

FIG. 9. Seasonal evolution of zonal mean (160°W–180°) SST (°C) from June(0) to June(1) during the 1997/98 El Niño event for the (a) EX_AC and (b) EX_NO_AC experiments.
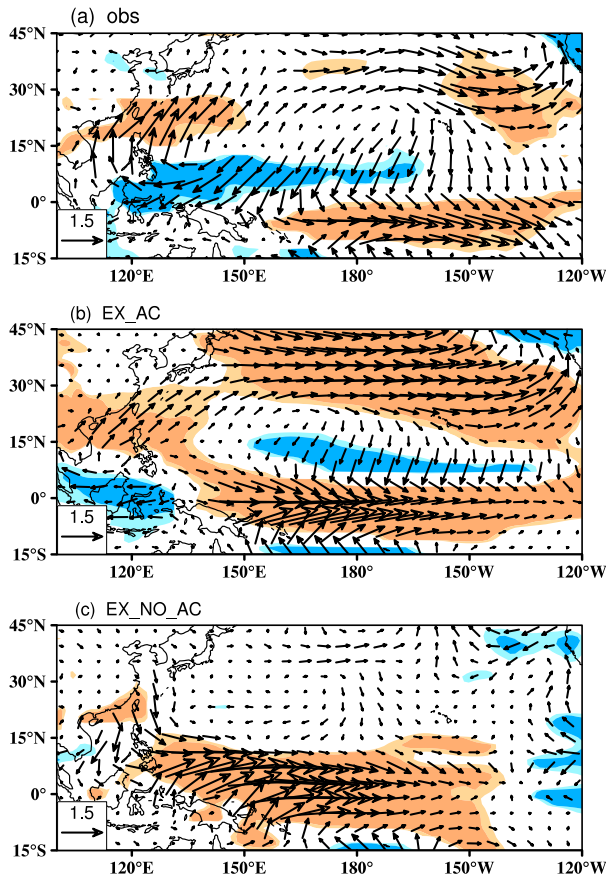
FIG. 10. Composite FMAM surface wind anomalies (m s^{-1}) during the El Niño decaying phase for the (a) observations, (b) EX_AC experiment, and (c) EX_NO_AC experiment. Light (dark) yellow and blue shadings indicate westerly and easterly anomalies exceeding the 90% (95%) confidence level, respectively.

FIG. 11. Composite monthly evolution of sea level pressure anomalies (hPa) over the Philippine Sea (10°–20°N, 120°–150°E) during El Niño events.

1997/98 El Niño event (Fig. 9b). Differences in this SST latitude–time evolution clearly indicate that the southward shift of the total SSTs is dependent on the seasonal cycle of climatological SST, which is very similar to the observations (Zhang et al. 2015).

Figure 10 shows the composite surface wind anomalies during the strong El Niño decaying phase for the observations and the two experiments. For the experiment including the annual cycle of SST (EX_AC), the atmospheric model realistically simulates two dominant observed features during the El Niño decaying phase: one is the southward shift of the CP zonal wind anomalies and the other is the strong anticyclonic circulation anomaly over the WNP region (Figs. 10a,b). This wind anomaly pattern is very similar to that of EOF2 (Fig. 1b). In the northwestern section of the anomalous WNP anticyclone, northeastward wind anomalies prevail over East Asia, which bring more water vapor from the south to China (Figs. 10a and 7b). In contrast to the
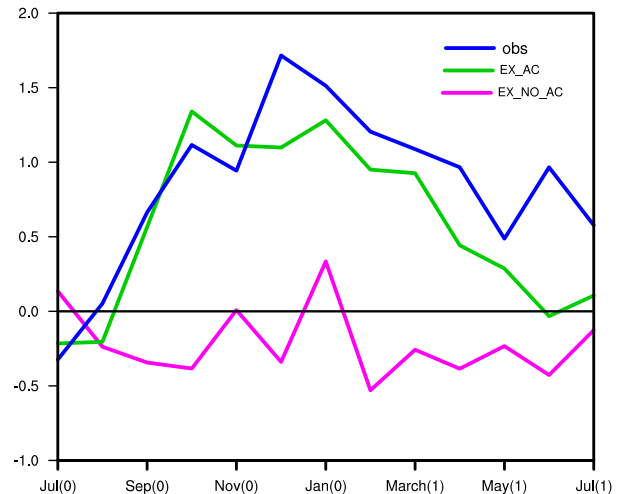
EX_AC experiment, no obvious meridional movement of the CP zonal wind anomalies is found in the EX_NO_ AC experiment (Fig. 10c). In this experiment, the cold and warm SST anomalies are, respectively, specified over the WNP and Indian Ocean, which have been argued to be important for the occurrence of the WNP anticyclonic anomalies in previous studies (e.g., Wang et al. 2000; Xie et al. 2009). However, no significant WNP anticyclonic circulation anomaly is seen in our experiment when the annual cycle of SST is excluded (Fig. 10c). This shows that the SST annual cycle is the crucial necessary condition for the development of the anomalous low-level WNP circulation.

We also examine the sea level pressure (SLP) anomaly evolution over the Philippine Sea (10°–20°N, 120°–150°E) associated with strong El Niño events (Fig. 11), following the area definition of Wang et al. (2000). The observed Philippine Sea SLP anomalies stay negative before the autumn season of El Niño developing phase and then rapidly reverse their sign around September of year 0 [September(0)]. Higher-than-normal SLP anomalies over the Philippine Sea persist for three or four seasons into the El Niño decaying summer (Fig. 11). The EX_AC experiment exhibits a similar Philippine Sea SLP anomaly evolution to the observations. In contrast to the EX_AC experiment, there are no positive SLP anomalies developing over the Philippine Sea in the EX_NO_AC simulation. Figures 10 and 11 highlight the importance of the SST annual cycle for the formation of the WNP anticyclonic anomalies during El Niño conditions. Contrasting the atmospheric response in these two experiments, we expect to find very different precipitation anomalies over eastern China. Indeed,
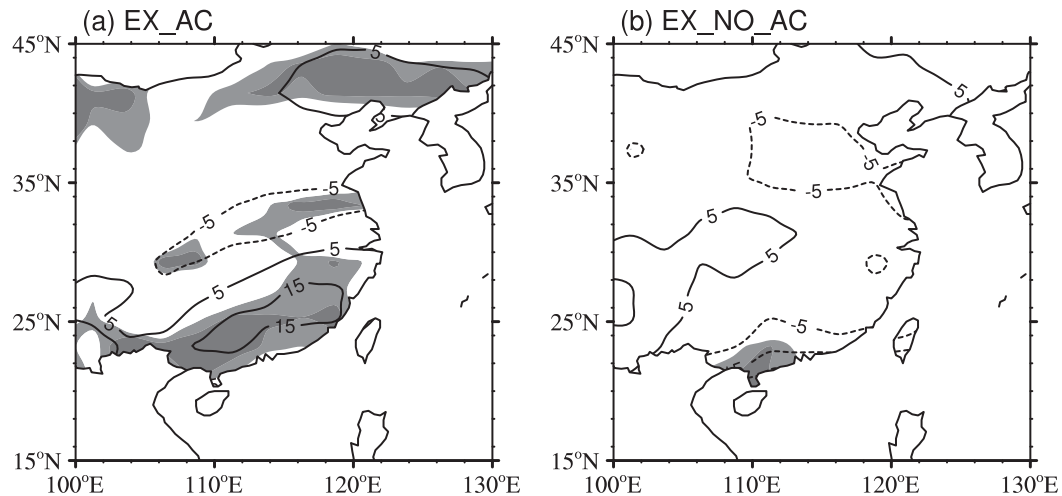
FIG. 12. Composite FMAM precipitation anomalies during the El Niño decaying phase for the (a) EX_AC and (b) EX_NO_AC experiments. Light (dark) shading denotes values exceeding the 80% (90%) confidence level.

in the EX_AC experiment, we find that southern China receives stronger precipitation anomalies during the El Niño decaying phase (Fig. 12a), consistent with the observations (Fig. 3). Northern China experiences different precipitation anomalies from the observations, possibly due to too strong impacts from the midlatitudes in the model and/or model biases in simulating the WNP circulation. However, in the EX_NO_AC experiment, no statistically significant precipitation anomalies can be found even over southern China (Fig. 12b), consistent with the absence of the anomalous WNP anticyclonic circulation in this experiment. Comparisons of the two modeling experiments verify our hypothesis that ENSO SST variability itself and its associated circulation pattern, without interaction with the annual cycle (C-mode), cannot give rise to the observed WNP atmospheric circulation anomalies and their associated precipitation anomalies over East Asia.

5. Conclusions and discussion

Southern China usually receives enhanced precipitation during the decaying phases of El Niño events and many studies have proposed various possible mechanisms as to how ENSO affects the East Asian climate (e.g., Zhang et al. 1996; Wang et al. 2000; Yang et al. 2007; Xie et al. 2009). In this study, we emphasize the key role of the SST seasonal cycle in the genesis of the ENSO-related climate anomalies over East Asia. It is shown that the direct (independent of the annual cycle) atmospheric response to the ENSO mode does not generate any statistically significant climate anomaly over East Asia, although it can give rise to climate

anomalies over the midlatitude regions via atmospheric teleconnections (e.g., the PNA pattern). In the tropical Pacific and adjacent continents, the direct ENSO signal is confined to the equatorial region and does not expand meridionally toward, for instance, the East Asian region. The C-mode, resulting from the interaction between interannual ENSO variability and the seasonal cycle of SST and circulation, is the key player in enhancing precipitation over southern China during the decaying phase of El Niño. As an important feature of the C-mode, strong anticyclonic low-level circulation anomalies are observed over the WNP region, which act to transport warm and moist water vapor to East Asia from the equatorial oceanic region. Our numerical model experiments reproduce well the key features of the anomalous WNP circulation during the El Niño decaying phase when including the SST annual cycle. However, no statistically significant WNP atmospheric circulation anomaly and thus no precipitation anomalies over southern China are generated when the SST boundary forcing is fixed to September equinox conditions (no annual cycle). As mentioned previously, the C-mode provides the crucial bridge to bring ENSO impacts to the off-equatorial region (e.g., southern China). Furthermore, we emphasize that the C-mode also provides a bridge in the spectral domain: the impacts of ENSO in these regions are characterized not only by the interannual ENSO time scale but most importantly by near-annual combination tones [see discussion in Stuecker et al. (2013, 2015) for details]. This key spectral feature of the C-mode has been overlooked in many previous climate impact studies by filtering out the near-annual variability and only focusing on the interannual frequency band.

Previous studies proposed that the WNP SST cooling and delayed Indian Ocean warming (both due to air–sea interaction) are the key mechanisms in forcing the WNP anticyclonic circulation anomalies during the El Niño decaying phase (e.g., Wang et al. 2000; Yang et al. 2007; Xie et al. 2009). In our simulations, the anomalous WNP circulation cannot be produced when the annual cycle is omitted, although the WNP SST cooling and Indian Ocean warming are included in the experimental SST anomaly boundary forcing. Stuecker et al. (2015) argued that the WNP anticyclonic circulation anomalies are predominantly a result of the southward shift of increased convection anomalies, which could induce subsidence over the WNP through a meridional circulation. In recent decades, steady progress has been made in simulating the key observed features of El Niño (e.g., AchutaRao and Sperber 2002, 2006; Guilyardi 2006; Randall et al. 2007; Zhang and Jin 2012). However, many studies demonstrate the existence of systematic errors in the simulated mean state and annual cycle (e.g., van Oldenborgh et al. 2005; Capotondi et al. 2006; Guilyardi 2006; Guilyardi et al. 2009; Wittenberg et al. 2006). These biases may cause large problems in simulating the regional climate responses of El Niño, even if we simulate a relatively realistic El Niño as defined by its anomalous evolution. This suggests that the climate community should pay close attention to the simulation of both realistic ENSO variability and the annual cycle in order to be able to simulate the El Niño–associated regional climate anomalies.

REFERENCES

AchutaRao, K., and K. R. Sperber, 2002: Simulation of the El Niño Southern Oscillation: Results from the Coupled Model Intercomparison Project. *Climate Dyn.*, **19**, 191–209, doi:10.1007/s00382-001-0221-9.

——, and ——, 2006: ENSO simulation in coupled ocean–atmosphere models: Are the current models better? *Climate Dyn.*, **27**, 1–15, doi:10.1007/s00382-006-0119-7.

Alexander, M. A., I. Bladé, M. Newman, J. R. Lanzante, N.-C. Lau, and J. D. Scott, 2002: The atmospheric bridge: The influence of ENSO teleconnections on air–sea interaction over the global oceans. *J. Climate*, **15**, 2205–2231, doi:10.1175/1520-0442(2002)015<2205:TABTIO>2.0.CO;2.

Anderson, J. L., and Coauthors, 2004: The new GFDL global atmosphere and land model AM2-LM2: Evaluation with prescribed SST simulations. *J. Climate*, **17**, 4641–4673, doi:10.1175/JCLI-3223.1.

Annamalai, H., P. Liu, and S.-P. Xie, 2005: Southwest Indian Ocean SST variability: Its local effect and remote influence on Asian monsoons. *J. Climate*, **18**, 4150–4167, doi:10.1175/JCLI3533.1.

Ashok, K., S. K. Behera, S. A. Rao, H. Y. Weng, and T. Yamagata, 2007: El Niño Modoki and its possible teleconnection. *J. Geophys. Res.*, **112**, C11007, doi:10.1029/2006JC003798.

Bjerknes, J., 1969: Atmospheric teleconnections from the equatorial Pacific. *Mon. Wea. Rev.*, **97**, 163–172, doi:10.1175/1520-0493(1969)097<0163:ATFTEP>2.3.CO;2.

Capotondi, A., A. Wittenberg, and S. Masina, 2006: Spatial and temporal structure of tropical Pacific interannual variability in 20th century coupled simulations. *Ocean Modell.*, **15**, 274–298, doi:10.1016/j.ocemod.2006.02.004.

Charney, J. G., and J. Shukla, 1981: Predictability of monsoons. *Monsoon Dynamics*, Sir James Lighthill and R. P. Pearce, Eds., Cambridge University Press, 99–109.

Feng, J., and J. Li, 2011: Influence of El Niño Modoki on spring rainfall over south China. *J. Geophys. Res.*, **116**, D13102, doi:10.1029/2010JD015160.

——, L. Wang, W. Chen, S. K. Fong, and K. C. Leong, 2010: Different impacts of two types of Pacific Ocean warming on Southeast Asia rainfall during boreal winter. *J. Geophys. Res.*, **115**, D24122, doi:10.1029/2010JD014761.

Fu, C. B., and X. L. Teng, 1988: Relationship between summer climate in China and El Niño/Southern Oscillation phenomenon (in Chinese). *Chin. J. Atmos. Sci.*, **12**, 133–141.

Gill, A. E., 1980: Some simple solutions for heat-induced tropical circulation. *Quart. J. Roy. Meteor. Soc.*, **106**, 447–462, doi:10.1002/qj.49710644905.

Guilyardi, E., 2006: El Niño–mean state–seasonal cycle interactions in a multi-model ensemble. *Climate Dyn.*, **26**, 329–348, doi:10.1007/s00382-005-0084-6.

——, A. Wittenberg, A. Fedorov, M. Collins, C. Wang, A. Capotondi, G. J. van Oldenborgh, and T. Stockdale, 2009: Understanding El Niño in ocean–atmosphere general circulation models. *Bull. Amer. Meteor. Soc.*, **90**, 325–340, doi:10.1175/2008BAMS2387.1.

Harrison, D. E., 1987: Monthly mean island surface winds in the central tropical Pacific and El Niño events. *Mon. Wea. Rev.*, **115**, 3133–3145, doi:10.1175/1520-0493(1987)115<3133:MMISWI>2.0.CO;2.

——, and N. K. Larkin, 1996: The COADS sea level pressure signal: A near-global El Niño composite and time series view, 1946–1993. *J. Climate*, **9**, 3025–3055, doi:10.1175/1520-0442(1996)009<3025:TCSLPS>2.0.CO;2.

——, and ——, 1998: El Niño–Southern Oscillation sea surface temperature and wind anomalies, 1946–1993. *Rev. Geophys.*, **36**, 353–399, doi:10.1029/98RG00715.

——, and G. A. Vecchi, 1999: On the termination of El Niño. *Geophys. Res. Lett.*, **26**, 1593–1596, doi:10.1029/1999GL900316.

Huang, R., and Y. Wu, 1989: The influence of ENSO on the summer climate change in China and its mechanism. *Adv. Atmos. Sci.*, **6**, 21–32, doi:10.1007/BF02656915.

Kalnay, E., and Coauthors, 1996: The NCEP/NCAR 40-Year Reanalysis Project. *Bull. Amer. Meteor. Soc.*, **77**, 437–471, doi:10.1175/1520-0477(1996)077<0437:TNYRP>2.0.CO;2.

Kao, H. Y., and J. Y. Yu, 2009: Contrasting eastern-Pacific and central-Pacific types of ENSO. *J. Climate*, **22**, 615–632, doi:10.1175/2008JCLI2309.1.

Karori, M. A., J. Li, and F.-F. Jin, 2013: The asymmetric influence of the two types of El Niño and La Niña on summer rainfall over southeast China. *J. Climate*, **26**, 4567–4582, doi:10.1175/JCLI-D-12-00324.1.

Kug, J.-S., I.-S. Kang, and S.-I. An, 2003: Symmetric and anti-symmetric mass exchanges between the equatorial and off-equatorial Pacific associated with ENSO. *J. Geophys. Res.*, **108**, 3284, doi:10.1029/2002JC001671.

——, F.-F. Jin, and S.-I. An, 2009: Two types of El Niño events: Cold tongue El Niño and warm pool El Niño. *J. Climate*, **22**, 1499–1515, doi:10.1175/2008JCLI2624.1.

Larkin, N. K., and D. E. Harrison, 2005: On the definition of El Niño and associated seasonal average U.S. weather anomalies. *Geophys. Res. Lett.*, **32**, L13705, doi:10.1029/2005GL022738.

Lau, N.-C., and M. J. Nath, 2006: ENSO modulation of the interannual and intraseasonal variability of the East Asian monsoon—A model study. *J. Climate*, **19**, 4508–4530, doi:10.1175/JCLI3878.1.

——, and ——, 2009: A model investigation of the role of air–sea interaction in the climatological evolution and ENSO-related variability of the summer monsoon over the South China Sea and western North Pacific. *J. Climate*, **22**, 4771–4792, doi:10.1175/2009JCLI2758.1.

Lengaigne, M., J. Boulanger, C. Meinkes, and H. Spencer, 2006: Influence of the seasonal cycle on the termination of El Niño events in a coupled general circulation model. *J. Climate*, **19**, 1850–1868, doi:10.1175/JCLI3706.1.

Li, T., Y. C. Tung, and J. W. Hwu, 2005: Remote and local SST forcing in shaping Asian–Australian monsoon anomalies. *J. Meteor. Soc. Japan*, **83**, 153–167, doi:10.2151/jmsj.83.153.

Matsuno, T., 1966: Quasi-geostrophic motion in the equatorial area. *J. Meteor. Soc. Japan*, **44**, 25–43.

McGregor, S., A. Timmermann, N. Schneider, M. F. Stuecker, and M. H. England, 2012: The effect of the South Pacific convergence zone on the termination of El Niño events and the meridional asymmetry of ENSO. *J. Climate*, **25**, 5566–5586, doi:10.1175/JCLI-D-11-00332.1.

——, N. Ramesh, P. Spence, M. H. England, M. J. McPhaden, and A. Santoso, 2013: Meridional movement of wind anomalies during ENSO events and their role in event termination. *Geophys. Res. Lett.*, **40**, 749–754, doi:10.1002/grl.50136.

Neelin, J. D., D. S. Battisti, A. C. Hirst, F.-F. Jin, Y. Wakata, T. Yamagata, and S. E. Zebiak, 1998: ENSO theory. *J. Geophys. Res.*, **103**, 14 261–14 290, doi:10.1029/97JC03424.

North, G. R., T. L. Bell, B. F. Cahalan, and F. J. Moeng, 1982: Sampling errors in the estimation of empirical orthogonal functions. *Mon. Wea. Rev.*, **110**, 699–706, doi:10.1175/1520-0493(1982)110<0699:SEITEO>2.0.CO;2.

Ohba, M., and H. Ueda, 2009: Role of nonlinear atmospheric response to SST on the asymmetric transition process of ENSO. *J. Climate*, **22**, 177–192, doi:10.1175/2008JCLI2334.1.

Randall, D. A., and Coauthors, 2007: Climate models and their evaluation. *Climate Change 2007: The Physical Science Basis*, S. Solomon et al., Eds., Cambridge University Press, 589–662.

Rayner, N. A., D. E. Parker, E. B. Horton, C. K. Folland, L. V. Alexander, D. P. Rowell, E. C. Kent, and A. Kaplan, 2003: Global analyses of sea surface temperature, sea ice, and night marine air temperature since the late nineteenth century. *J. Geophys. Res.*, **108**, 4407, doi:10.1029/2002JD002670.

Ren, H.-L., and F.-F. Jin, 2011: Niño indices for two types of ENSO. *Geophys. Res. Lett.*, **38**, L04704, doi:10.1029/2010GL046031.

Ropelewski, C. F., and M. S. Halpert, 1987: Global and regional scale precipitation patterns associated with the El Niño/Southern Oscillation. *Mon. Wea. Rev.*, **115**, 1606–1626, doi:10.1175/1520-0493(1987)115<1606:GARSPP>2.0.CO;2.

——, and ——, 1996: Quantifying Southern Oscillation–precipitation relationships. *J. Climate*, **9**, 1043–1059, doi:10.1175/1520-0442(1996)009<1043:QSOPR>2.0.CO;2.

Spencer, H., 2004: Role of the atmosphere in seasonal phase locking of El Niño. *Geophys. Res. Lett.*, **31**, L24104, doi:10.1029/2004GL021619.

Stuecker, M. F., A. Timmermann, F.-F. Jin, S. McGregor, and H.-L. Ren, 2013: A combination mode of the annual cycle and the El Niño/Southern Oscillation. *Nat. Geosci.*, **6**, 540–544, doi:10.1038/ngeo1826.

——, F.-F. Jin, A. Timmermann, and S. McGregor, 2015: Combination mode dynamics of the anomalous northwest Pacific anticyclone. *J. Climate*, **28**, 1093–1111, doi:10.1175/JCLI-D-14-00225.1.

Tao, S., and Y. Ding, 1981: Observational evidence of the influence of the Qinghai-Xizang (Tibet) Plateau on the occurrence of heavy rain and severe convective storms in China. *Bull. Amer. Meteor. Soc.*, **62**, 23–30, doi:10.1175/1520-0477(1981)062<0023:OEOTIO>2.0.CO;2.

Trenberth, K. E., and J. M. Caron, 2000: The Southern Oscillation revisited: Sea level pressure, surface temperatures, and precipitation. *J. Climate*, **13**, 4358–4365, doi:10.1175/1520-0442(2000)013<4358:TSORSL>2.0.CO;2.

van Loon, H., and R. A. Madden, 1981: The Southern Oscillation. Part I: Global associations with pressure and temperature in northern winter. *Mon. Wea. Rev.*, **109**, 1150–1162, doi:10.1175/1520-0493(1981)109<1150:TSOPIG>2.0.CO;2.

van Oldenborgh, G. J., S. Philip, and M. Collins, 2005: El Niño in a changing climate: A multi-model study. *Ocean Sci.*, **1**, 81–95, doi:10.5194/os-1-81-2005.

Vecchi, G., and D. E. Harrison, 2003: On the termination of the 2002–03 El Niño event. *Geophys. Res. Lett.*, **30**, 1964, doi:10.1029/2003GL017564.

——, and ——, 2006: The termination of the 1997/98 El Niño. Part I: Mechanisms of oceanic change. *J. Climate*, **19**, 2633–2646, doi:10.1175/JCLI3776.1.

Wallace, J. M., E. M. Rasmusson, T. P. Mitchell, V. E. Kousky, E. S. Sarachik, and H. Von Storch, 1998: On the structure and evolution of ENSO-related climate variability in the tropical Pacific: Lessons from TOGA. *J. Geophys. Res.*, **103**, 14 241–14 259, doi:10.1029/97JC02905.

Wang, B., and Q. Zhang, 2002: Pacific–East Asian teleconnection. Part II: How the Philippine Sea anomalous anticyclone is established during El Niño development. *J. Climate*, **15**, 3252–3265, doi:10.1175/1520-0442(2002)015<3252:PEATPI>2.0.CO;2.

——, R. Wu, and X. Fu, 2000: Pacific–East Asian teleconnection: How does ENSO affect East Asian climate? *J. Climate*, **13**, 1517–1536, doi:10.1175/1520-0442(2000)013<1517:PEATHD>2.0.CO;2.

——, Q. Bao, B. Hoskins, G. Wu, and Y. Liu, 2008: Tibetan Plateau warming and precipitation change in East Asia. *Geophys. Res. Lett.*, **35**, L14702, doi:10.1029/2008GL034330.

——, B. Xiang, and J.-Y. Lee, 2013: Subtropical high predictability establishes a promising way for monsoon and tropical storm predictions. *Proc. Natl. Acad. Sci. USA*, **110**, 2718–2722, doi:10.1073/pnas.1214626110.

Wang, C., and X. Wang, 2013: Classifying El Niño Modoki I and II by different impacts on rainfall in southern China and typhoon tracks. *J. Climate*, **26**, 1322–1338, doi:10.1175/JCLI-D-12-00107.1.

Watanabe, M., and F.-F. Jin, 2002: Role of Indian Ocean warming in the development of Philippine Sea anticyclone during ENSO. *Geophys. Res. Lett.*, **29** (10), doi:10.1029/2001GL014318.

——, and ——, 2003: A moist linear baroclinic model: Coupled dynamical–convective response to El Niño. *J. Climate*, **16**, 1121–1139, doi:10.1175/1520-0442(2003)16<1121:AMLBMC>2.0.CO;2.

Weng, H., K. Ashok, S. K. Behera, S. A. Rao, and T. Yamagata, 2007: Impacts of recent El Niño Modoki on dry/wet conditions in the Pacific rim during boreal summer. *Climate Dyn.*, **29**, 113–129, doi:10.1007/s00382-007-0234-0.

Wittenberg, A. T., A. Rosati, N. C. Lau, and J. J. Ploshay, 2006: GFDL's CM2 global coupled climate models. Part III: Tropical Pacific climate and ENSO. *J. Climate*, **19**, 698–722, doi:10.1175/JCLI3631.1.

Wu, B., T. Li, and T. Zhou, 2010: Relative contributions of the Indian Ocean and local SST anomalies to the maintenance of the western North Pacific anomalous anticyclone during the El Niño decaying summer. *J. Climate*, **23**, 2974–2986, doi:10.1175/2010JCLI3300.1.

Wu, G., and H. Liu, 1995: Neighborhood response of rainfall to tropical sea surface temperature anomalies. Part I: Numerical experiment. *Chin. J. Atmos. Sci.*, **19**, 422–434.

Wu, R., and Z. Z. Hu, 2003: Evolution of ENSO-related rainfall anomalies in East Asia. *J. Climate*, **16**, 3742–3758, doi:10.1175/1520-0442(2003)016<3742:EOERAI>2.0.CO;2.

——, and B. P. Kirtman, 2007: Observed relationship of spring and summer East Asian rainfall with winter and spring Eurasian snow. *J. Climate*, **20**, 1285–1304, doi:10.1175/JCLI4068.1.

Wu, T.-W., and Z.-A. Qian, 2003: The relation between the Tibetan winter snow and the Asian summer monsoon and rainfall: An observational investigation. *J. Climate*, **16**, 2038–2051, doi:10.1175/1520-0442(2003)016<2038:TRBTTW>2.0.CO;2.

Wu, Z., B. Wang, J. Li, and F.-F. Jin, 2009: An empirical seasonal prediction model of the East Asian summer monsoon using ENSO and NAO. *J. Geophys. Res.*, **114**, D18120, doi:10.1029/2009JD011733.

——, J. Li, Z. Jiang, and T. Ma, 2012: Modulation of the Tibetan Plateau snow cover on the ENSO teleconnections: From the East Asian summer monsoon perspective. *J. Climate*, **25**, 2481–2489, doi:10.1175/JCLI-D-11-00135.1.

Xiang, B., B. Wang, and T. Li, 2013: A new paradigm for predominance of standing central Pacific warming after the late 1990s. *Climate Dyn.*, **41**, 327–340, doi:10.1007/s00382-012-1427-8.

Xie, F., J. Li, W. Tian, J. Feng, and Y. Huo, 2012: Signals of El Niño Modoki in the tropical tropopause layer and stratosphere. *Atmos. Chem. Phys.*, **12**, 5259–5273, doi:10.5194/acp-12-5259-2012.

——, ——, ——, Y. Li, and J. Feng, 2014a: Indo-Pacific warm pool area expansion, Modoki activity, and tropical cold-point tropopause temperature variations. *Sci. Rep.*, **4**, 4552, doi:10.1038/srep04552.

——, ——, ——, J. Zhang, and J. Shu, 2014b: The impacts of two types of El Niño on global ozone variations in the last three decades. *Adv. Atmos. Sci.*, **31**, 1113–1126, doi:10.1007/s00376-013-3166-0.

Xie, S. P., K. Hu, J. Hafner, H. Tokinaga, Y. Du, G. Huang, and T. Sampe, 2009: Indian Ocean capacitor effect on Indo-western Pacific climate during the summer following El Niño. *J. Climate*, **22**, 730–747, doi:10.1175/2008JCLI2544.1.

Yang, J., Q. Liu, S. P. Xie, Z. Liu, and L. Wu, 2007: Impact of the Indian Ocean SST basin mode on the Asian summer monsoon. *Geophys. Res. Lett.*, **34**, L02708, doi:10.1029/2006GL028571.

Ye, D., 1981: Some characteristics of the summer circulation over the Qinghai-Xizang (Tibet) Plateau and its neighborhood. *Bull. Amer. Meteor. Soc.*, **62**, 14–19, doi:10.1175/1520-0477(1981)062<0014:SCOTSC>2.0.CO;2.

Yeh, S.-W., J.-S. Kug, B. Dewitte, M.-H. Kwon, B. P. Kirtman, and F.-F. Jin, 2009: El Niño in a changing climate. *Nature*, **461**, 511–514, doi:10.1038/nature08316.

Yuan, Y., S. Yang, and Z. Zhang, 2012: Different evolutions of the Philippine Sea anticyclone between the eastern and central Pacific El Niño: Possible effects of Indian Ocean SST. *J. Climate*, **25**, 7867–7883, doi:10.1175/JCLI-D-12-00004.1.

Zhang, R., A. Sumi, and M. Kimoto, 1996: Impact of El Niño on the East Asian monsoon: A diagnostic study of the '86/87 and '91/92 events. *J. Meteor. Soc. Japan*, **74**, 49–62.

——, ——, and ——, 1999: A diagnostic study of the impact of El Niño on the precipitation in China. *Adv. Atmos. Sci.*, **16**, 229–241, doi:10.1007/BF02973084.

Zhang, W., and F.-F. Jin, 2012: Improvements in the CMIP5 simulations of ENSO-SSTA meridional width. *Geophys. Res. Lett.*, **39**, L23704, doi:10.1029/2012GL053588.

——, ——, J. Li, and H.-L. Ren, 2011: Contrasting impacts of two-type El Niño over the western North Pacific. *J. Meteor. Soc. Japan*, **89**, 563–569, doi:10.2151/jmsj.2011-510.

——, ——, J. X. Zhao, L. Qi, and H.-L. Ren, 2013: The possible influence of a non-conventional El Niño on the severe autumn drought of 2009 in southwest China. *J. Climate*, **26**, 8392–8405, doi:10.1175/JCLI-D-12-00851.1.

——, ——, and A. Turner, 2014: Increasing autumn drought over southern China associated with ENSO regime shift. *Geophys. Res. Lett.*, **41**, 4020–4026, doi:10.1002/2014GL060130.

——, H. Li, F.-F. Jin, M. Stuecker, A. Turner, and N. Klingamam, 2015: The annual-cycle modulation of meridional asymmetry in ENSO's atmospheric response and its dependence on ENSO zonal structure. *J. Climate*, **28**, 5795–5812, doi:10.1175/JCLI-D-14-00724.1.

Zhang, Y., T. Li, and B. Wang, 2004: Decadal change of the spring snow depth over the Tibetan Plateau: The associated circulation and influence on the East Asian summer monsoon. *J. Climate*, **17**, 2780–2793, doi:10.1175/1520-0442(2004)017<2780:DCOTSS>2.0.CO;2.